# Introduction to Optical Modeling and Design

Frank Wyrowski

# Chapter 1

# Modeling and design of lens systems

by *Uwe Zeitner* introduces e.g.:

- Introduction to ray tracing
- Paraxial approximation / Gaussian optics
- ABCD-system matrix formalism
- Brief consideration of physical optics propagation into focus of lens

In what follows we like to extend those concepts by:

- Propagation of electromagnetic fields and not only rays.
- No restriction to propagation through lenses but also for instance scatterer and diffractive elements.
- Inclusion of physical optics free-space propagation.

# Chapter 2

# Representation of electromagnetic fields

In what follows an overview of basic facts on the representation and nature of monochromatic electromagnetic fields in homogeneous dielectrics is given.

## 2.1 Maxwell's equations in frequency domain

- We consider electromagnetic fields in a linear, homogeneous, isotropic, non-absorbing dielectric, which is characterized by the refractive index $n(\omega) = \sqrt{\epsilon_{\mathrm{r}}(\omega)}$.

- We use a complex amplitude representation of the field components in the frequency domain.

- Then the electric field $\boldsymbol{E} = (E_x, E_y, E_z)$ and the magnetic field $\boldsymbol{H} = (H_x, H_y, H_z)$ are governed by the following Maxwell's equations:

$$\nabla \times \boldsymbol{E}(\boldsymbol{r};\omega) = \mathrm{i}\omega\mu_0\boldsymbol{H}(\boldsymbol{r};\omega) \tag{2.1}$$

$$\nabla \times \boldsymbol{H}(\boldsymbol{r};\omega) = -\mathrm{i}\omega\epsilon_0\epsilon_{\mathrm{r}}(\omega)\boldsymbol{E}(\boldsymbol{r};\omega)\,, \tag{2.2}$$

$$\nabla \cdot \boldsymbol{E}(\boldsymbol{r};\omega) = 0\,, \tag{2.3}$$

$$\nabla \cdot \boldsymbol{H}(\boldsymbol{r};\omega) = 0\,. \tag{2.4}$$

- From these Maxwell's equations the Helmholtz' equation can be concluded:

$$\nabla^2\boldsymbol{E}(\boldsymbol{r};\omega) + \frac{\omega^2}{c^2}\epsilon_{\mathrm{r}}(\omega)\boldsymbol{E}(\boldsymbol{r};\omega) = 0 \tag{2.5}$$

- The same result is valid for the magnetic field. Equation (2.5) can be read componentwise. Thus, each field component of $\boldsymbol{H}$ and $\boldsymbol{E}$ must satisfy the Helmholtz equation.

- Typically we concentrate on fields with one frequency $\omega_0$ only, which are called monochromatic or harmonic fields.

- There are several ways to introduce harmonic fields mathematically. [1]

- We define a harmonic field by its complex version in the frequency domain, that is [2]

$$\boldsymbol{E}(\boldsymbol{r};\omega) = \boldsymbol{E}(\boldsymbol{r})\delta(\omega-\omega_0) \tag{2.6}$$

with the complex amplitude

$$\boldsymbol{E}(\boldsymbol{r}) = \begin{bmatrix} |E_x(\boldsymbol{r})|\exp[\mathrm{i}\phi_x(\boldsymbol{r})] \\ |E_y(\boldsymbol{r})|\exp[\mathrm{i}\phi_y(\boldsymbol{r})] \\ |E_z(\boldsymbol{r})|\exp[\mathrm{i}\phi_z(\boldsymbol{r})] \end{bmatrix} . \tag{2.7}$$

[1] Comment on stationary: Monochromatic fields are stationary. Polychromatic fields can be stationary, e.g. sun light, or non-stationary, e.g. fs pulses.

[2] Though we concentrate on the electric field, the same is valid for the magnetic one.

- Inverse Fourier transformation of (2.6) yields the complex harmonic electric field

$$\boldsymbol{\mathsf{E}}(\boldsymbol{r};t) = \boldsymbol{E}(\boldsymbol{r})\exp\left(-\mathrm{i}\omega_0 t\right) \quad . \tag{2.8}$$

  in time domain.

- The real electric field is obtained by taking the real part and we obtain

$$\boldsymbol{\mathsf{E}}_{\mathrm{r}}(\boldsymbol{r};t) = \Re\big[\boldsymbol{E}(\boldsymbol{r})\exp(-\mathrm{i}\omega_0 t)\big] = \begin{bmatrix} |E_x(\boldsymbol{r})|\cos[\phi_x(\boldsymbol{r}) - \omega_0 t] \\ |E_y(\boldsymbol{r})|\cos[\phi_y(\boldsymbol{r}) - \omega_0 t] \\ |E_z(\boldsymbol{r})|\cos[\phi_z(\boldsymbol{r}) - \omega_0 t] \end{bmatrix} . \tag{2.9}$$

- If we restrict Maxwell's equations to one monochromatic solution (frequency $\omega_0$)we obtain equations for the complex amplitudes by

$$\nabla \times \boldsymbol{E}(\boldsymbol{r}) = \mathrm{i}\omega_0\mu_0\boldsymbol{H}(\boldsymbol{r}) \tag{2.10}$$
$$\nabla \times \boldsymbol{H}(\boldsymbol{r}) = -\mathrm{i}\omega_0\epsilon_0\epsilon_{\mathrm{r}}(\omega_0)\boldsymbol{E}(\boldsymbol{r})\,, \tag{2.11}$$
$$\nabla \cdot \boldsymbol{E}(\boldsymbol{r}) = 0\,, \tag{2.12}$$
$$\nabla \cdot \boldsymbol{H}(\boldsymbol{r}) = 0\,. \tag{2.13}$$

- These equations constitute the basis for all following considerations.

## 2.2 Plane waves

### 2.2.1 Definition and properties

- Let us now consider the complex amplitude vector of a harmonic field of the form

$$\boldsymbol{E}(\boldsymbol{r}) = \boldsymbol{E}_0 \exp(\mathrm{i}\tilde{\boldsymbol{k}} \cdot \boldsymbol{r}) \tag{2.14}$$

with the so-called complex wave vector

$$\tilde{\boldsymbol{k}} = \boldsymbol{k}' + \mathrm{i}\boldsymbol{k}'' \tag{2.15}$$

with real valued vectors $\boldsymbol{k}'$ and $\boldsymbol{k}''$.

- Analogously to (2.14) the magnetic field is defined by

$$\boldsymbol{H}(\boldsymbol{r}) = \boldsymbol{H}_0 \exp(\mathrm{i}\tilde{\boldsymbol{k}} \cdot \boldsymbol{r}) \,. \tag{2.16}$$

- It is straightforward to show, that $\boldsymbol{E}(\boldsymbol{r})$ and $\boldsymbol{H}(\boldsymbol{r})$ are componentwise solutions of Helmholtz' equation provided that

$$\tilde{\boldsymbol{k}}^2(\omega) = \omega^2 n^2(\omega)/c^2 = k_0^2 n^2(\omega) \tag{2.17}$$

is satisfied.[3]

[3] We will see later, that though the right side of the equation is real valued, the wave vector on the left can be complex valued.

- The wave number in vacuum is denoted by $k_0 = \omega/c$. From $\nu\lambda = c$ and $\omega = 2\pi\nu$ follows $k_0 = 2\pi/\lambda$. Equation (2.17) is called the dispersion relation, because it relates the wave number vector $\tilde{\boldsymbol{k}}$ in media with the frequency $\omega$.

- Next we reformulate Eq. (2.14) and obtain

$$\boldsymbol{E}(\boldsymbol{r}) = \boldsymbol{E}_0 \exp(\mathrm{i}\boldsymbol{k}' \cdot \boldsymbol{r}) \exp(-\boldsymbol{k}'' \cdot \boldsymbol{r}) \tag{2.18}$$

  using (2.15).

- The first factor governs the phase front $\boldsymbol{k}' \cdot \boldsymbol{r} =$ constant, which is obviously a plane equation. The second factor does the same for the magnitude of the field.

- In general both planes are not parallel and the waves are called inhomogeneous. If both planes are parallel, the field is called a homogeneous plane wave.

- It should be noted, that $|\boldsymbol{k}''| = 0$ is a sufficient condition to obtain a homogeneous wave.

- The magnetic field is always related to the electric field via (2.1) and that specifies

$\boldsymbol{H}_0$ of (2.16) according to

$$\boldsymbol{H}_0 = \sqrt{\frac{\varepsilon_0}{\mu_0}} \frac{\tilde{\boldsymbol{k}} \times \boldsymbol{E}_0}{k} \,. \tag{2.19}$$

- Moreover, equation (2.3) must be satisfied which leads to $\tilde{\boldsymbol{k}} \cdot \boldsymbol{E}_0 = 0$ and therefore $\tilde{\boldsymbol{k}} \perp \boldsymbol{E}_0$.
- Analogously (2.4) yields $\tilde{\boldsymbol{k}} \perp \boldsymbol{H}_0$. $\boldsymbol{E}_0 \perp \boldsymbol{H}_0$ follows from (2.19).
- All this together leads to the result, that plane waves are always transversal. This result is only valid for plane waves!
- The vector cross product in (2.19) is defined by

$$\tilde{\boldsymbol{k}} \times \boldsymbol{E}_0 = \begin{vmatrix} \hat{\boldsymbol{x}} & \hat{\boldsymbol{y}} & \hat{\boldsymbol{z}} \\ \tilde{k}_x & \tilde{k}_y & \tilde{k}_z \\ E_{0,x} & E_{0,y} & E_{0,z} \end{vmatrix} \tag{2.20}$$

with the unit direction vectors $\hat{\boldsymbol{x}}$, $\hat{\boldsymbol{y}}$ and $\hat{\boldsymbol{z}}$. That gives in detail

$$\begin{aligned} \tilde{\boldsymbol{k}} \times \boldsymbol{E}_0 = {} & (\tilde{k}_y \, E_{0,z} - \tilde{k}_z \, E_{0,y})\hat{\boldsymbol{x}} \\ & + (\tilde{k}_z \, E_{0,x} - \tilde{k}_x \, E_{0,z})\hat{\boldsymbol{y}} + (\tilde{k}_x \, E_{0,y} - \tilde{k}_y \, E_{0,x})\hat{\boldsymbol{z}} \,. \end{aligned} \tag{2.21}$$

- Because of (2.3) it becomes clear, that not all of the components of $\boldsymbol{E}_0$ can be chosen independently.

- Indeed it follows directly

$$E_{z,0} = -\frac{\tilde{k}_x E_{x,0} + \tilde{k}_y E_{y,0}}{\tilde{k}_z} \,. \tag{2.22}$$

- Thus we come to the extremely important result: The six field components of plane waves are completely described in any homogeneous and isotropic medium in 3D by the two components $E_{x,0}$ and $E_{y,0}$ for a given wave vector $\tilde{\boldsymbol{k}}$.

### 2.2.2 Discussion of dispersion relation

- Because of the dispersion relation (2.17) also the three components of $\tilde{\boldsymbol{k}}$ are not independent.

- Typically $\tilde{k}_z$ is considered to be dependent of $\tilde{k}_x$ and $\tilde{k}_y$ and according to the dispersion relation with $\tilde{\boldsymbol{k}}(\omega) \cdot \tilde{\boldsymbol{k}}(\omega) = \tilde{k}_x^2 + \tilde{k}_y^2 + \tilde{k}_z^2$ we may write

$$\tilde{k}_z^2 = k_0^2 n^2 - (\tilde{k}_x^2 + \tilde{k}_y^2) \,. \tag{2.23}$$

- In our discussion we are in particular interested in plane waves with real valued $\tilde{k}_x$ and $\tilde{k}_y$ components, that is $k_x, k_y \in \Re$. Then it follows

$$\tilde{k}_z^2 = k_0^2 n^2 - (k_x^2 + k_y^2)\,. \tag{2.24}$$

- That results in

$$\tilde{k}_z = \begin{cases} \sqrt{k_0^2 n^2 - (k_x^2 + k_y^2)} & k_x^2 + k_y^2 \leq k_0^2 n^2 \\ \mathrm{i}\sqrt{(k_x^2 + k_y^2) - k_0^2 n^2} & k_x^2 + k_y^2 > k_0^2 n^2 \end{cases}\,. \tag{2.25}$$

- Thus we have solutions with real valued $\tilde{k}_z$ (upper branch) and a pure imaginary $\tilde{k}_z$ (lower branch).

- Application of the definition in Eq. (2.15) on Eq. (2.25) leads to the two cases:

  1. $k_x^2 + k_y^2 \leq k_0^2 n^2$: $\boldsymbol{k}' = \boldsymbol{k}$ and $\boldsymbol{k}'' = 0$, that is the $\tilde{\boldsymbol{k}}$-vector is real-valued.

  2. $k_x^2 + k_y^2 > k_0^2 n^2$: $\boldsymbol{k}' = (k_x, k_y, 0)$ and $\boldsymbol{k}'' = (0, 0, \sqrt{k_x^2 + k_y^2 - k_0^2 n^2})$

- In the first case the plane waves are homogeneous and in the second case inhomogeneous ($\boldsymbol{k}' \perp \boldsymbol{k}''$), which have the special name evanescent plane waves.

- The positive root is used to formulate (2.25). It ensures decaying evanescent fields and propagating fields in positive $z$-direction.
- The second case shows, that Eq. (2.17) can also be satisfied when $\tilde{\boldsymbol{k}}$ has complex-valued components.
- The $1/e$-propagation distance $z_e$ of the evanescent fields is given, acccording to the second factor in Eq. (2.18), by

$$z_e(k_x, k_y) = \frac{1}{\sqrt{k_x^2 + k_y^2 - k_0^2 n^2}} \,. \tag{2.26}$$

- It is often helpful, to describe the real valued solution of the wave vector in spherical coordinates and that means

$$\boldsymbol{k} = k_0 n \hat{\boldsymbol{k}} = k_0 n \left(\sin\theta\cos\phi, \sin\theta\sin\phi, \cos\theta\right) \tag{2.27}$$

with the unit direction vector $\hat{\boldsymbol{k}} = \boldsymbol{k}/|\boldsymbol{k}|$.

- That also allows a discussion of the meaning of the two branches in (2.25). To this end we evaluate $k_x^2 + k_y^2 \leq k_0^2 n^2$.

- Substituting (2.27) leads to

$$\begin{aligned} k_x^2 + k_y^2 &= k_0^2 n^2 (\sin^2\theta\cos^2\phi + \sin^2\theta\sin^2\phi) \\ &= k_0^2 n^2 \sin^2\theta \le k_0^2 n^2 \end{aligned} \tag{2.28}$$

- That leads to the trivial result $-1 \le \sin\theta \le 1$. Thus the threshold between propagating and evanescent fields is obviously identical with the condition $|\theta| \le 90^o$.

- In conclusion, in a dielectric medium plane fields which propagate in the positive $z$-direction are homogeneous for angles $\theta$ up to 90 degrees. Then the waves become evanescent and do approximately (see Eq. (2.26)) not propagate anymore. Nevertheless evanescent fields are very important in near field interaction.

## 2.3 Angular spectrum of plane waves (SPW)

### 2.3.1 Decomposition of fields by plane waves

- In optical modeling we often consider light fields on planes $\Upsilon$. Next we discuss how to decompose an arbitrary harmonic field in a homogeneous medium on such a plane into a set of plane waves.

- Let us describe an arbitrary component ($\boldsymbol{E}$ and $\boldsymbol{H}$) of the harmonic field which propagates in $+z$-direction on the plane $\Upsilon$ with $V(\boldsymbol{\rho}; \omega)$.
- Thereby we use the position vector $\boldsymbol{\rho} = (x, y)$ in the local coordinate system of $\Upsilon$ which is defined with the origin in $\Upsilon$. Thus $z = 0$ in this coordinate system and we may skip it. Moreover we skip the frequency $\omega$ in what follows.
- Formally we may introduce the **spatial** Fourier transformation of $V(\boldsymbol{\rho})$ in form of

$$A(\boldsymbol{\kappa}) = \mathcal{F}V(\boldsymbol{\rho}) = \frac{1}{2\pi} \int\int_{-\infty}^{\infty} V(\boldsymbol{\rho})\, \mathrm{e}^{-\mathrm{i}\boldsymbol{\kappa}\cdot\boldsymbol{\rho}}\, \mathrm{d}^2\rho \tag{2.29}$$

  with the real-valued $\boldsymbol{\kappa} = (k_x, k_y)$.
- The related inverse Fourier transformation is given by

$$V(\boldsymbol{\rho}) = \mathcal{F}^{-1}A(\boldsymbol{\kappa}) = \frac{1}{2\pi} \int\int_{-\infty}^{\infty} A(\boldsymbol{\kappa})\, \mathrm{e}^{+\mathrm{i}\boldsymbol{\kappa}\cdot\boldsymbol{\rho}}\, \mathrm{d}^2\kappa\,. \tag{2.30}$$

- Comparison of the integral kernel with the plane wave exponential term $\exp[\mathrm{i}(k_x\, x + k_y\, y + \tilde{k}_z\, z]$ for the wave vectors of the form (2.24) shows, that (2.30) can be interpreted as the decomposition of $V(\boldsymbol{\rho})$ into plane waves in $z = 0$ with the amplitudes $A(\boldsymbol{\kappa})$ per spatial-frequency vector $\boldsymbol{\kappa}$.

- $\tilde{k}_z$ is function of $\boldsymbol{\kappa}$ according to the dispersion relation of plane waves in homogeneous media. We know its specific form for dielectrics without damping from (2.25).
- That shows, that the plane wave decomposition of fields in dielectrics without damping includes propagating and evanescent plane waves.
- Equation (2.30) is typically referred to as spectrum of plane waves (SPW) decomposition and it is valid for any component of $\boldsymbol{E}$ and $\boldsymbol{H}$. However we know, that for plane waves the field components are not independent. That is essential for the further discussion.

### 2.3.2 SPW representation of electric field

- Next we discuss the SPW representation of the electric field components including the dependency between them.
- Let us consider the complex amplitude components of the electric field in the plane $\Upsilon$, that is

$$\boldsymbol{E}(\boldsymbol{\rho}) = \Big(E_x(\boldsymbol{\rho}), E_y(\boldsymbol{\rho}), E_z(\boldsymbol{\rho})\Big) . \tag{2.31}$$

- For each of them we can calculate the SPW amplitudes by

$$A_\ell(\boldsymbol{\kappa}) = \mathcal{F}\, V_\ell(\boldsymbol{\rho}) \tag{2.32}$$

according to (2.29) with $\ell = 1, 2, 3$ for the $x$, $y$ and $z$ components of the electric field in space and $k$-domain, that are for instance $V_1 = E_x$ and $A_2 = \mathcal{F}\, E_y$.

- Let us assume that we know $E_x$ and $E_y$ and via Fourier transformation $A_1$ and $A_2$. $A_1(\boldsymbol{\kappa})$ and $A_2(\boldsymbol{\kappa})$ are the amplitudes of plane waves propagating into the direction which is specified by $\boldsymbol{\kappa}$.

- Thus, we know through (2.22) that the complex amplitude $A_3$ depends directly from the others and we find

$$A_3(\boldsymbol{\kappa}) = -\frac{k_x A_1(\boldsymbol{\kappa}) + k_y A_2(\boldsymbol{\kappa})}{\tilde{k}_z}\,. \tag{2.33}$$

- Because of (2.32) we also have

$$A_3(\boldsymbol{\kappa}) = \mathcal{F} E_z(\boldsymbol{\rho})\,. \tag{2.34}$$

- By setting the right sides of both equations equal we find

$$\mathcal{F} E_z(\boldsymbol{\rho}) = -\frac{k_x A_1(\boldsymbol{\kappa}) + k_y A_2(\boldsymbol{\kappa})}{\tilde{k}_z} \tag{2.35}$$

which can be resolved for $E_z$. That results, by using (2.32) for $\ell = 1, 2$, in

$$E_z(\boldsymbol{\rho}) = -\boldsymbol{\mathcal{F}}^{-1}\left\{\frac{1}{\tilde{k}_z}\Big(k_x\boldsymbol{\mathcal{F}}\,E_x(\boldsymbol{\rho}) + k_y\boldsymbol{\mathcal{F}}E_y(\boldsymbol{\rho})\Big)\right\}. \tag{2.36}$$

- Equation (2.36) formulates an algorithm to calculate $E_z$ on $\Upsilon$ for given $E_x$ and $E_y$ on $\Upsilon$.
- Comment: Intuitive explanation by plane wave sketch at board.
- Important conclusion: The electric field is completely specified on a plane $\Upsilon$ which is situated in a homogeneous medium by determining $E_x(\boldsymbol{\rho})$ and $E_y(\boldsymbol{\rho})$ in this plane. The $z$-component is redundant and can be calculated on demand!
- VirtualLab$^{\text{TM}}$ Simulation electric field.

### 2.3.3 SPW representation of magnetic field

- Let us next consider the complex amplitude of the magnetic field on the plane $\Upsilon$, that is

$$\boldsymbol{H}(\boldsymbol{\rho}) = \Big(H_x(\boldsymbol{\rho}), H_y(\boldsymbol{\rho}), H_z(\boldsymbol{\rho})\Big). \tag{2.37}$$

- We can calculate for each of them the corresponding SPW component via

$$A_\ell(\boldsymbol{\kappa}) = \mathcal{F}\, V_\ell(\boldsymbol{\rho}) \tag{2.38}$$

with $\ell = 4, 5, 6$ for the $x$, $y$ and $z$ components of the magnetic field in both domains.

- Because the $A_\ell$ for $\ell = 4, 5, 6$ are the magnetic field amplitudes of plane waves we conclude from (2.19)

$$\boldsymbol{A}_H(\boldsymbol{\kappa}) = \frac{1}{k}\sqrt{\frac{\varepsilon_0}{\mu_0}}\, \tilde{\boldsymbol{k}} \times \boldsymbol{A}_E(\boldsymbol{\kappa}) \tag{2.39}$$

with $\boldsymbol{A}_H = \Big(A_4(\boldsymbol{\kappa}), A_5(\boldsymbol{\kappa}), A_6(\boldsymbol{\kappa})\Big)$ and $\boldsymbol{A}_E = \Big(A_1(\boldsymbol{\kappa}), A_2(\boldsymbol{\kappa}), A_3(\boldsymbol{\kappa})\Big)$.

- In detail we find via (2.21)

$$A_4 = \frac{1}{k}\sqrt{\frac{\varepsilon_0}{\mu_0}}(k_y A_3 - \tilde{k}_z A_2) \tag{2.40}$$

$$A_5 = \frac{1}{k}\sqrt{\frac{\varepsilon_0}{\mu_0}}(\tilde{k}_z A_1 - k_x A_3) \tag{2.41}$$

$$A_6 = \frac{1}{k}\sqrt{\frac{\varepsilon_0}{\mu_0}}(k_x A_2 - k_y A_1) \tag{2.42}$$

where we have skipped the arguments of the SPW components.

- Substituting $A_3$ of (2.33) leads to:

$$A_4 = -\frac{1}{k}\sqrt{\frac{\varepsilon_0}{\mu_0}}\frac{1}{\tilde{k}_z}\left[k_x k_y A_1 + (k_y^2 + \tilde{k}_z^2)A_2\right] \tag{2.43}$$

$$A_5 = -\frac{1}{k}\sqrt{\frac{\varepsilon_0}{\mu_0}}\frac{1}{\tilde{k}_z}\left[(k_x^2 + \tilde{k}_z^2)A_1 + k_x k_y A_2\right] \tag{2.44}$$

$$A_6 = \frac{1}{k}\sqrt{\frac{\varepsilon_0}{\mu_0}}\left(k_x A_2 - k_y A_1\right) \tag{2.45}$$

- Equalizing the right-handed sides of (2.38) and (2.43) - (2.45) and resolving for the magnetic field components results in:

$$\begin{aligned} H_x(\boldsymbol{\rho}) = -\frac{1}{k}\sqrt{\frac{\varepsilon_0}{\mu_0}}\,\boldsymbol{\mathcal{F}}^{-1}\Big\{\frac{1}{\tilde{k}_z}\Big[&k_x k_y \boldsymbol{\mathcal{F}} E_x(\boldsymbol{\rho}) \\ &+ (k_y^2 + \tilde{k}_z^2)\boldsymbol{\mathcal{F}} E_y(\boldsymbol{\rho})\Big]\Big\}, \end{aligned} \tag{2.46}$$

$$H_y(\boldsymbol{\rho}) = -\frac{1}{k}\sqrt{\frac{\varepsilon_0}{\mu_0}}\,\boldsymbol{\mathcal{F}}^{-1}\Big\{\frac{1}{\tilde{k}_z}\Big[(k_x^2+\tilde{k}_z^2)\boldsymbol{\mathcal{F}}E_x(\boldsymbol{\rho}) + k_x k_y \boldsymbol{\mathcal{F}}E_y(\boldsymbol{\rho})\Big]\Big\} \tag{2.47}$$

and

$$H_z(\boldsymbol{\rho}) = \frac{1}{k}\sqrt{\frac{\varepsilon_0}{\mu_0}}\,\boldsymbol{\mathcal{F}}^{-1}\Big\{k_x\boldsymbol{\mathcal{F}}E_y(\boldsymbol{\rho}) - k_y\boldsymbol{\mathcal{F}}E_x(\boldsymbol{\rho})\Big\}\,. \tag{2.48}$$

- It follows, that the magnetic field on $\Upsilon$ can be completely calculated from given $E_x(\boldsymbol{\rho})$ and $E_y(\boldsymbol{\rho})$.

- VirtualLab$^{\mathrm{TM}}$ Simulation magnetic field.

- In conclusion, the harmonic field on a plane boundary $\Upsilon$ in a homogeneous media is completely specified by specification of the $x$- and $y$-components of the electric field on $\Upsilon$.

## 2.4 Polarization

- In general we may define: A light field is fully polarized, if the tip of the electric field vector $\boldsymbol{E}(\boldsymbol{r};t)$ moves on a time independent loop in space at any location $\boldsymbol{r}$.

- It is very important to know, that light is still polarized, if the loop changes with the location $\boldsymbol{r}$.

- Instead we speak about partially polarized light, if the movement of the tip occurs along some walk in space which changes in time in a more or less random-like way.

- In case of completely unpolarized light, the vector moves along a random walk in all locations $\boldsymbol{r}$.

- Polarization is a 3D phenomenon of electromagnetic fields, because the vector of the electric field is a 3D vector whose components change in time.

- Harmonic fields are always polarized! That follows directly from its definition in the time domain according to eq. (2.9), that is

$$\boldsymbol{E}_{\mathrm{r}}(\boldsymbol{r};t) = \Re\big[\boldsymbol{E}(\boldsymbol{r})\exp(-\mathrm{i}\omega_0 t)\big] = \begin{bmatrix} |E_x(\boldsymbol{r})|\cos[\phi_x(\boldsymbol{r}) - \omega_0 t] \\ |E_y(\boldsymbol{r})|\cos[\phi_y(\boldsymbol{r}) - \omega_0 t] \\ |E_z(\boldsymbol{r})|\cos[\phi_z(\boldsymbol{r}) - \omega_0 t] \end{bmatrix} . \tag{2.49}$$

- It defines an ellipse in 3D, which depends on the location $\boldsymbol{r}$ via the magnitude and phase values. (Show polarization.pdf file with figures; internship.)
- Often we consider the projection of this ellipse into one plane only, that are the $xy$-, $zx$- and $zy$-planes.
- Then just two of the three components contribute to the curve, which becomes an ellipse in the plane.
- The special cases are circles and straight lines, which are called circularly and linearly polarized light.
- It is emphasized, that the parameters of the ellipses depend on the location $\boldsymbol{r}$ and the projection plane. In conclusion, harmonic fields are typically locally polarized.
- For paraxial fields the $z$-component has very small magnitude in comparison to the other two components. Then, polarization can be discussed in the $xy$-plane only.

- Often globally polarized, paraxial harmonic fields are considered. On a plane $\Upsilon$ they are defined by

$$\Big(E_x(\boldsymbol{\rho}), E_y(\boldsymbol{\rho})\Big) = \boldsymbol{J}\; U(\boldsymbol{\rho}) \tag{2.50}$$

  with the constant Jones vector $\boldsymbol{J} = (J_x, J_y)$.

- Obviously for fields of the form (2.50) the state of polarization in the $xy$-projection plane is invariant of the location $\boldsymbol{\rho}$. Sometimes this type of polarization is also called uniformly polarized.

- Warning: Even if Eq. (2.50) is satisfied, but the field is NOT paraxial, then the field cannot be understood as globally polarized, because the 3D polarization ellipses changes in space. That means globally polarization is a useful concept for paraxial light only.

- VirtualLab$^{\mathrm{TM}}$ illustration of cases shown before!

## 2.5 Conclusion

- We have learned how to represent an electromagnetic field in a plane which resides in a homogeneous dielectric (without damping).
- By specifying the $x$- and $y$-components of the electric field, the other four field components can be calculated on demand.
- Next we turn to the propagation of vectorial electromagnetic fields from one plane to another one, that is to the question on how to obtain 3D field information from a given 2D one.

# Chapter 3

# Tracing operators in matrix formalism

## 3.1 General operator matrix

- Let us consider a situation as it is illustrated in Fig. 8.1. We are interested in a mathematical description of the propagation from the input plane $\Upsilon^{\mathrm{in}}$ to output plane $\Upsilon^{\mathrm{out}}$ which are both placed in homogeneous media.

- The field tracing operation from the input to the output plane is mathematically described by the matrix operator equation

$$\boldsymbol{V}^{\mathrm{out}} = \boldsymbol{\mathcal{C}}\boldsymbol{V}^{\mathrm{in}} \tag{3.1}$$

  with the tracing operator $\boldsymbol{\mathcal{C}}$.

- The harmonic fields in both planes are completely specified by the $x$- and $y$-components of the electric field.
- Conclusion: The field tracing operator equation (3.1) can be formally reduced to those components and we obtain the matrix equation

$$\left\{\begin{bmatrix} E_x \\ E_y \end{bmatrix}^{\text{out}}\right\}_{\Upsilon^{\text{out}}} = \begin{bmatrix} \mathcal{C}_{xx} & \mathcal{C}_{xy} \\ \mathcal{C}_{yx} & \mathcal{C}_{yy} \end{bmatrix} \left\{\begin{bmatrix} E_x \\ E_y \end{bmatrix}^{\text{in}}\right\}_{\Upsilon^{\text{in}}} . \tag{3.2}$$

- Here we use local coordinate systems for the input and output field vectors, which is denoted by the curls. Then, the operator must include the coordinate transformation also. For a general 3D system modeling this situation is typical (sketch at board).
- However, often we consider parallel planes and then we obtain the matrix equation

$$\begin{bmatrix} E_x(\boldsymbol{\rho}, z) \\ E_y(\boldsymbol{\rho}, z) \end{bmatrix} = \begin{bmatrix} \mathcal{C}_{xx} & \mathcal{C}_{xy} \\ \mathcal{C}_{yx} & \mathcal{C}_{yy} \end{bmatrix} \begin{bmatrix} E_x(\boldsymbol{\rho}, 0) \\ E_y(\boldsymbol{\rho}, 0) \end{bmatrix} . \tag{3.3}$$

- Obviously, in general a field tracing operator has a significant influence on the polarization of the input field.
- $\mathcal{C}_{xx}$ and $\mathcal{C}_{yy}$ change the incident components directly.

- $\mathcal{C}_{xy}$ and $\mathcal{C}_{yx}$ mathematically describe crosstalk between the two components.
- Some operator matrices, as for example the propagation matrix for propagation through homogeneous media (see Ch. 5), are of the special diagonal form with $\mathcal{C} = \mathcal{C}_{xx} = \mathcal{C}_{yy}$ and $\mathcal{C}_{xy} = \mathcal{C}_{yx} = 0$, that results in

$$\boldsymbol{\mathcal{C}} = \mathcal{C} \begin{bmatrix} 1 & 0 \\ 0 & 1 \end{bmatrix} = \mathcal{C}\boldsymbol{\mathcal{I}} \tag{3.4}$$

  with the identity matrix $\boldsymbol{\mathcal{I}}$ and the operator $\mathcal{C}$.
- We refer to propagation operator matrices of the form Eq. (3.4) as *diagonal type operator matrix*.
- Next we consider the special case of a globally polarized input field

$$\begin{bmatrix} E_x(\boldsymbol{\rho}, 0) \\ E_y(\boldsymbol{\rho}, 0) \end{bmatrix} = \begin{bmatrix} J_x \\ J_y \end{bmatrix}^{\text{in}} U(\boldsymbol{\rho}, 0) = \boldsymbol{J}^{\text{in}} U(\boldsymbol{\rho}, 0)\,, \tag{3.5}$$

  with the Jones vector $\boldsymbol{J}^{\text{in}}$ and its complex numbers $J_x$ and $J_y$.
- Let us assume the propagation is of the diagonal form of Eq. (3.4). Then we obtain the output field

$$\boldsymbol{J}^{\text{in}} U(\boldsymbol{\rho}, z) = \boldsymbol{J}^{\text{in}} \mathcal{C} U(\boldsymbol{\rho}, 0)\,. \tag{3.6}$$

- The *global* polarization is not affected by this operator. Therefore, if a system can be modeled by a diagonal type operator, then the Jones vector is not affected and can be skipped in all formulas. Only in this case just the scalar field $U$ appears in the modeling equations.

- However, that is not an approximation as long as diagonal type operator matrix models the system with high accuracy. We will see, that this is the case in particular in paraxial systems.

- It should be emphasized:

  - The polarization in the $xy$-plane is not affected by a diagonal type operator matrix for globally polarized input fields only.

  - However the distribution $U(\boldsymbol{\rho}, z)$ is changed in comparison to the one in $z = 0$ and thus also the resulting $z$-component $E_z$ is changed even in the case of an operator of type Eq. (3.4).

  - In case of a non-paraxial field that results in a change of the polarization in the $xz$- and $yz$-planes.

  - Only in case of globally polarized AND paraxial fields a vectorial effect of the diagonal type operator matrix can be neglected and a pure scalar effect is obtained.

- Equations (3.2) and (3.3) include all effects on the input field.
- VirtualLab™ Illustration of propagation effects on polarizaion.

## 3.2 Jones matrices

- Sometimes it is sufficient to discuss the vectorial effect only and to neglect the real 3D wave propagation.
- This is in particular the case for thin components and anisotropic media inside of them, e.g. a $\lambda/4$-plate or a stress-induced birefrigent effect. Then it is often sufficient to model the effect on the polarization of the harmonic field only.
- Mathematically that means:

$$\boldsymbol{\mathcal{C}}(\boldsymbol{\rho}) = \boldsymbol{\mathcal{J}}(\boldsymbol{\rho}) = \begin{bmatrix} J_{xx}(\boldsymbol{\rho}) & J_{xy}(\boldsymbol{\rho}) \\ J_{yx}(\boldsymbol{\rho}) & J_{yy}(\boldsymbol{\rho}) \end{bmatrix} \tag{3.7}$$

  with complex valued functions $J_{\alpha\beta}(\boldsymbol{\rho})$ for $\alpha = x, y$ and $\beta = x, y$.

- This matrix is typically called *generalized Jones matrix*. They are for instance of concern to describe vectorial effects inside of laser resonators. Such matrices introduce a locally polarized field even for a globally polarized input field.
- VirtualLab$^{\mathrm{TM}}$ Illustration of the effect of generalized Jones matrices.
- Often the general case is more simplified by laterally independent components of the generalized Jones matrix.
- In that case the components are simple complex numbers and one obtains

$$\boldsymbol{\mathcal{J}} = \begin{bmatrix} J_{xx} & J_{xy} \\ J_{yx} & J_{yy} \end{bmatrix} , \tag{3.8}$$

  which is referred to as *Jones matrix*.
- Obviously, in case of globally polarized input fields the Jones vector is changed only.
- For locally polarized input fields not only the polarization is changed but typically also the lateral field distribution.
- Trivial example: Donut mode and polarizer in $x$-direction. Result: Hermite-Gaussian mode (1,0) as $y$-component and zero $x$-component.

- VirtualLab™ Illustration of the effect of Jones matrices.

# Chapter 4

# Field tracing by geometrical optics

As introduction PowerPoint “From ray to field tracing”.

## 4.1 Ray tracing

### 4.1.1 Basics of ray tracing

- Ray tracing is based on the Local Plane Wave Approximation (LPWA) (see Fig. 8.3).
- If we consider an electromagnetic field in space, it is to some approximation possible to interpret the field locally in a position $\boldsymbol{r}$ by a plane wave:

$$\boldsymbol{E}^{\mathrm{LPW}}(\boldsymbol{r}') = \boldsymbol{E}_0^{\mathrm{LPW}}(\boldsymbol{r}) \exp[\mathrm{i}k_0 n(\lambda)\hat{\boldsymbol{k}}(\boldsymbol{r}) \cdot \boldsymbol{r}'] \tag{4.1}$$

- Obviously, a local plane wave is defined by the following quantities:
  - $\lambda$
  - Position vector $\boldsymbol{r}$
  - Refractive index $n$ at position $\boldsymbol{r}$
  - Complex amplitude $\boldsymbol{E}_0^{\mathrm{LPW}}(\boldsymbol{r})$
  - Direction unit vector $\hat{\boldsymbol{k}}(\boldsymbol{r})$
- Ray tracing can be understood as the propagation of the local plane wave according to the laws of plane wave propagation.

- Diffraction effects due to the limited extent of the local plane wave are neglected, that means it is a geometrical optics approximation.
- In particular one can exploit the following rigorously solved tracing situations:
  - Plane wave propagation through a plane interface.
  - Plane wave propagation through a grating.
- If the ray hits an interface between two media, locally a plane interface is assumed (Local Plane Interface Approximation; LPIA) and locally a plane wave/plane interface interaction is modeled.
- Analogously it is possible to formulate a Local Linear Grating Approximation (LLGA). See Fig. 8.4.
- Generally we describe the effect on a local plane wave at a boundary by **boundary operators**.
- We distinguish between basic and vectorial ray tracing:

  **Basic Ray Tracing** Only the positions $\boldsymbol{r}$ and directions $\hat{\boldsymbol{k}}(\boldsymbol{r})$ are considered.

  **Vectorial Ray Tracing** Besides positions and directions also the change of the complex amplitude of the local plane wave at boundaries are taken into account.

### 4.1.2 Boundary operator

- Let us next discuss the effect of a boundary operator on the LPW. We assume for the sake of simplicity, that all quantities are defined in the same coordinate system. In practice, the use of local coordinate systems is often required.
- Boundary operators are defined by the following rules, which are applied at the position $\boldsymbol{r}$ on the boundary.

**Position Rule** The boundary operator can change the position, at which the propagation of the LPW/ray is to be continued:

$$\boldsymbol{r} \longrightarrow \boldsymbol{r}^{\mathrm{BO}} \tag{4.2}$$

At a simple interface we typically have $\boldsymbol{r} = \boldsymbol{r}^{\mathrm{BO}}$. Examples for changes of the position follow from interfaces with coatings or inclusion of Goos-Hänchen shift.

**Direction Rule** The change of the direction vector $\hat{\boldsymbol{k}}$ is defined by the direction rule:

$$\hat{\boldsymbol{k}}(\boldsymbol{r}) \longrightarrow \hat{\boldsymbol{k}}^{\mathrm{BO}}(\boldsymbol{r}^{\mathrm{BO}}) \tag{4.3}$$

**Complex Amplitude Rule** Besides the direction the complex amplitude is the major physical quantity of a LPW. The complex amplitude rule defines the change of the electric field vector (superscript LPW is skipped):

$$\boldsymbol{E}_0(\boldsymbol{r}) \longrightarrow \boldsymbol{E}_0^{\mathrm{BO}}(\boldsymbol{r}^{\mathrm{BO}}) \tag{4.4}$$

This rule is applied to the phase and amplitude of the two orthogonal and transversal field components in the local coordinate system.

- In addition we define the following characteristic of boundary operators: A boundary operator may define multiple sets of position, direction and complex amplitude rules. Then it generates also multiple outputs. For instance a boundary operator defines the effect on the transmitted and reflected LPW.
- Each boundary is related to exactly one boundary operator.
- In summary a ray tracing algorithm through a sequence of boundaries mainly consists of the following steps:
  1. LPWA: The incident field is locally interpreted by plane waves and the plane wave quantities are calculated accordingly.
  2. Ray Tracing Engine: The ray tracing engine finds the intersection points of the initial rays with the next boundary.

3. Boundary Operator: At the intersection point the local boundary operator is applied to the incident LPW.
4. The resulting LPW is used to trace to the next boundary.

- Vectorial ray tracing provides field values in any intersection point of a ray with the output plane.
- If we do that in a way which ensures proper sampling of the field in this plane we obtain geometrical optics field tracing. This is discussed in more detail in the lecture OMD I.
- Here we simplify the geometrical optics modeling significantly in order to obtain a very popular modeling technique in optics.

## 4.2 Thin Element Approximation (TEA)

### 4.2.1 Mathematical formulation

- In Fourier optics and various other fields of optics a special version of field tracing is the standard modeling approach. Free space propagation is modeled by wave optics and the propagation through optical components by the thin element approximation (TEA).
- The propagation through one optical interface of height profile $h(\boldsymbol{\rho})$ with TEA is illustrated in Fig. 8.2.
- Let us discuss this approach in terms of ray tracing as presented before in Sec. 4.1.
- The rays in TEA possesses the following characteristics:
  - The positions $\boldsymbol{\rho}$ of the LPW's lie on an equidistant grid.
  - The directions of all LPW's are parallel to the optical axis.
  - The boundary operator does not change the direction of the rays, that is refraction is neglected.
  - In conclusion the rays hit the output plane on the same equidistant grid as

in the input plane. That is numerically very convenient for the application of subsequent physical optics based propagation techniques in the output plane.

- Obviously the simple choice of the LPW directions and neglecting the refraction at the boundary is a very strong approximation.
- It is only justified, if the input field is paraxial. Then the assumption about the LPW directions makes sense.
- Neglecting refraction is only justified, if the interface is almost plane and orthogonal to the $z$-axis. In other words it means that the interface must be thin, which is the reason for the name TEA.
- In vectorial ray tracing we include the determination of the optical path length (and the absorption) along the rays.
- Mathematically it takes the following form: The optical path length OPL is calculated along the indicated rays and it follows the phase

$$\phi(\boldsymbol{\rho}) = k_0 \mathrm{OPL}(\boldsymbol{\rho}) = k_0(n - n')h(\boldsymbol{\rho}) + \phi_0 \tag{4.5}$$

with the constant phase $\phi_0 = k_0 n' h_0$.

- An effect on the amplitude is due to Fresnel losses (and energy considerations). However, the boundary operator amplitude rule of TEA does not include lateral variation of those effects and a constant factor is included only (and often even not taklen into account, if energy conversation must not be included in the modeling).

- In summary the TEA-operator takes the compact form

$$\begin{aligned} V_\ell^{\text{out}}(\boldsymbol{\rho}, h_0) &= \boldsymbol{\mathcal{C}}_{\text{TEA}} V_\ell^{\text{in}}(\boldsymbol{\rho}, 0) \\ &= t_{\text{Fresnel}}\, V_\ell^{\text{in}}(\boldsymbol{\rho}, 0)\ \mathrm{e}^{\mathrm{i}\phi(\boldsymbol{\rho})} \end{aligned} \tag{4.6}$$

  for $\ell = 1, 2$ and with $\phi(\boldsymbol{\rho})$ from Eq. (4.5).

- Though TEA is often understood as a scalar technique, here it is defined for the electric field components $E_x$ and $E_y$. The other components follow by the equations known in homogeneous media. This way TEA is formulated for a vectorial harmonic field.

- The TEA effect is the same for both field components and of course there is no crosstalk. Thus, the TEA operator matrix is of a diagonal form with the consequences discussed in Ch. 3.

- The numerical implementation of TEA is very simple. Starting from an equidistantly sampled $V_\ell^{\text{in}}(\boldsymbol{\rho}, 0)$ the operator $\boldsymbol{\mathcal{C}}_{\text{TEA}}$ is evaluated for any sampling point $\boldsymbol{\rho}_m$. This is a pointwise operation which leads to $V_\ell^{\text{out}}(\boldsymbol{\rho}, h_0)$.

- Though TEA is derived as a special geometrical optics approach, in practice TEA does not require a ray tracing step. That is because all quantities can be calculated directly for a given height profile $h(\boldsymbol{\rho})$. May be that is the reason that sometimes TEA is understood as a wave optical technique. However, that is absolutely not true. TEA is the lowest level geometrical optics approach.

- According to (4.6) the effect of TEA on the input field can be simply expressed by the multiplication of the transmission function

$$t(\boldsymbol{\rho}) = t_{\text{Fresnel}}\, \mathrm{e}^{\mathrm{i}\phi(\boldsymbol{\rho})}\,. \tag{4.7}$$

Such transmission functions are often used in Fourier optics and related fields.

- So far we discussed the calculation of the transmitted field by TEA. Analogously we may derive the TEA operator of the reflected field and obtain

$$V_\ell^{\text{out}}(\boldsymbol{\rho}, 0) = r_{\text{Fresnel}}\, V_\ell^{\text{in}}(\boldsymbol{\rho}, 0)\, \mathrm{e}^{\mathrm{i}\phi(\boldsymbol{\rho})} \tag{4.8}$$

with the Fresnel reflection coefficient $r$ and

$$\phi(\boldsymbol{\rho}) = 2k_0 n h(\boldsymbol{\rho})\,. \tag{4.9}$$

- TEA is widely used in optical modeling, e.g. in laser optics, diffractive optics, holography and Fourier optics. In particular in diffractive optics TEA is not only applied for modeling, but also for the design of micro-structured interfaces.
- By some design algorithm it follows, that a phase $\phi(\boldsymbol{\rho})$ should be impressed onto an incident field, in order to achieve some desired light distribution of the propagated field, e.g. beam splitting or shaping.
- Thus we deal with the inverse versions of Eqs. (4.5) and (4.9), which yields

$$h(\boldsymbol{\rho}) = \frac{\lambda}{2\pi\big(n(\lambda) - n'(\lambda)\big)}\phi(\boldsymbol{\rho}) \tag{4.10}$$

and

$$h(\boldsymbol{\rho}) = \frac{\lambda}{4\pi n(\lambda)}\phi(\boldsymbol{\rho}) \tag{4.11}$$

without taking constant phases into consideration. The maximum height level appears for $\phi = 2\pi$.

- Assuming $n = 1.5$ and $n' = 1$ we obtain $h(\boldsymbol{\rho}) \leq 2\lambda$ in case of transmission mode of operation and $h(\boldsymbol{\rho}) \leq \lambda/2$ in case of reflection with $n = 1$.
- Obviously, the resulting height profiles are very thin and as long as the lateral features are clearly larger than the wavelength TEA is a reasonable approach.
- Example linear phase transmission by sawtooth grating in TEA modeling!
- Remark: The design of the height profiles drastically depends on the wavelength. Thus, the resulting diffractive elements provide good performance only for the design wavelength.
- Rule of thumb: As long as the field in an optical system remains paraxial (divergence 1 degree and smaller) and the effect of all components can be modeled by a diagonal type operator matrix, TEA is often sufficient to model the propagation of fields through the components.
- Warning: However, then in free space full geometrical optics or physical optics propagation must be applied! Example: A lens modeling by TEA (see Sec. 4.2.2) with subsequent free space propagation by TEA would not result in any focusing effect.

- Conclusion: In practice TEA modeling of components is typicall combined with physical optics modeling between the components, see for example Fourier optics.

### 4.2.2 Example Thin Lens

- The most important interface in optical engineering is the spherical surface of radius $R$ illustrated in Fig. 8.5, with

$$h(\boldsymbol{\rho}) = h(x, y) = R - \left(R^2 - x^2 - y^2\right)^{1/2} . \tag{4.12}$$

- The radius of curvature $R$ of a surface is therefore taken to be:
  - Positive ($R > 0$) if the surface is convex (when viewed from the left)
  - Negative ($R < 0$) if the surface is concave

- In the paraxial approximation we can make use of the Taylor expansion in (4.12) to obtain

$$h(x, y) = \frac{x^2 + y^2}{2R} , \tag{4.13}$$

i.e., a parabolic profile. This profile may be used in the TEA equations for any paraxial input field.

- Let us next assume that a paraxial spherical wave (parabolic wave) with phase function ($\ell = 1, 2$; use index $i$ and $t$ for incident and transmitted field respectively)

$$\Phi_{\mathrm{i}}(x, y) = \Phi_{\mathrm{i}} + \frac{k_0 n_{\mathrm{i}}}{2R_{\mathrm{i}}}\left(x^2 + y^2\right) \ , \tag{4.14}$$

  where $R_{\mathrm{i}}$ is the radius of curvature at $z = 0$, is incident on the parabolic interface.

- The radius of wavefront for a spherical/parabolic wave which is propagating along the $z$-axis (to the right) is:
  - Positive ($R > 0$) for a diverging wave
  - Negative ($R < 0$) for a converging wave

- It should be noted, that the definition of the signs of the radii is inverse for the waves and the surfaces.

- According to Eq. (4.5) the transmitted wave is also a paraxial spherical wave with the phase function

$$\Phi_{\mathrm{t}}(x, y) = \Phi_{\mathrm{t}} + \frac{k_0 n_{\mathrm{t}}}{2R_{\mathrm{t}}}\left(x^2 + y^2\right) \ , \tag{4.15}$$

where the radius of curvature $R_\mathrm{t}$ is given by

$$\frac{n_\mathrm{t}}{R_\mathrm{t}} = \frac{n_\mathrm{i}}{R_\mathrm{i}} + \frac{n_\mathrm{i} - n_\mathrm{t}}{R} \tag{4.16}$$

and $\Phi_\mathrm{t} = \Phi_\mathrm{i} + \phi_0$ is a constant phase.

- Let us consider the signs for a special case:
  - Plane incident wave, that means $R_\mathrm{i} = \infty$
  - Convex surface, that means $R > 0$
  - $n_\mathrm{i} < n_\mathrm{t}$

  From these assumptions and Eq. (4.16) it follows $R_\mathrm{t} < 0$, that is we obtain a converging field as it is expected.

- Considering next a reflective instead of a transmissive interface, a similar procedure yields a parabolic reflected wave

$$\Phi_\mathrm{r}(x, y) = \Phi_\mathrm{r} + \frac{k_0 n_\mathrm{i}}{2R_\mathrm{r}} \left(x^2 + y^2\right) \; , \tag{4.17}$$

where

$$-\frac{1}{R_\mathrm{r}} = \frac{1}{R_\mathrm{i}} + \frac{2}{R} \tag{4.18}$$

~~and $\Phi_r = \Phi_i$~~.

- Let us finally consider a thin lens, which consists of two parabolic interfaces, with radii of curvature $R_1$ and $R_2$, in close proximity.
- The refractive index between the interfaces is assumed to be $n$ while the refractive index on both sides is $n = 1$.
- According to (4.16),

$$\frac{n}{R_L} = \frac{1}{R_i} + \frac{1-n}{R_1} , \tag{4.19}$$

where $R_L$ is the radius of wavefront curvature between the interfaces, and

$$\frac{1}{R_t} = \frac{n}{R_L} + \frac{n-1}{R_2} . \tag{4.20}$$

- Eliminating $R_L$ from (4.19) and (4.20) gives

$$\frac{1}{R_t} = \frac{1}{R_i} - \frac{1}{f} , \tag{4.21}$$

where

$$\frac{1}{f} = (n-1)\left(\frac{1}{R_1} - \frac{1}{R_2}\right) . \tag{4.22}$$

- From (4.21) follows $R_\mathrm{t} = -f$ for $R_\mathrm{i} = \infty$, that means a plane incident wave converges towards a point located at a distance $f$ behind the lens. Hence $f$ is called the focal length of the lens.
- Obviously Eq. (4.21) is nothing else as the thin lens equation when we replace the radii by distances.
- Moreover, Eq. (4.22) is the well-known lens-maker's formula.
- Mathematically the derivation mainly benefits from the paraxial/quadratic approximation and the simple multiplication rules for quadratic phase factors.

# Chapter 5

# Physical optics free-space propagation

## 5.1 Introduction

- Next we consider the propagation of harmonic fields through a homogeneous dielectric between two planes.
- The propagation of the field from a plane $\Upsilon_i$ to $\Upsilon_j$ can be formulated by
$$\boldsymbol{V}(\boldsymbol{r} \in \Upsilon_j) = \boldsymbol{\mathcal{P}}_{ij}\boldsymbol{V}(\boldsymbol{r} \in \Upsilon_i) \tag{5.1}$$
with the propagation operator $\boldsymbol{\mathcal{P}}_{ij}$.
- Let us formulate the problem in the local coordinate system of the plane $\Upsilon_i$ (with the origin at $z = 0$ in the plane $i$). Then, we find $\boldsymbol{V}(\boldsymbol{r} \in \Upsilon_i) = \boldsymbol{V}(\boldsymbol{\rho}, 0)$ with $\boldsymbol{\rho} = (x, y)$ in the local coordinate system.

- If we assume that both planes are parallel and have a distance $z$ then $\boldsymbol{V}(\boldsymbol{r} \in \Upsilon_j) = \boldsymbol{V}(\boldsymbol{\rho}, z)$ follows. The propagation problem in this coordinate system reads

$$\boldsymbol{V}(\boldsymbol{\rho}, z) = \boldsymbol{\mathcal{P}} \boldsymbol{V}(\boldsymbol{\rho}, 0) \tag{5.2}$$

  where we skipped the index $ij$ at the propagation operator.

- In order to develop a propagation operator $\boldsymbol{\mathcal{P}}$ we follow a very basic approach in optical modeling and design. We look for elementary solutions of the problem and try then to decompose the general problem into a set of the elementary one.

- Propagation of harmonic fields is often discussed in terms of Huygens' principle.

- In an electromagnetic sense it can be summarized as follows: Fist we solve the propagation problem for an arbitrary spherical harmonic field. Then we decompose the general harmonic field into spherical ones and apply the superposition principle.

- In scalar optics this approach is rather convenient. However, in electromagnetic theory, it suffers from the complexity of electromagnetic spherical fields.

- Thus we apply another approach, which is also very popular in optics and which in addition allows an electromagnetic approach conveniently. It is based on the

SPW decomposition of harmonic fields and we refer to it as the SPW propagation operator.

## 5.2 Spectrum of plane waves (SPW)

- The SPW decomposition of harmonic fields in plane $z = 0$ is given by (compare with (2.30))

$$V_\ell(\boldsymbol{\rho}, 0) = \mathcal{F}^{-1} A_\ell(\boldsymbol{\kappa}) = \frac{1}{2\pi} \int\!\!\int_{-\infty}^{\infty} A_\ell(\boldsymbol{\kappa})\, \mathrm{e}^{\mathrm{i}\boldsymbol{\kappa}\cdot\boldsymbol{\rho}}\, \mathrm{d}^2\kappa \tag{5.3}$$

for all components $\ell = 1, \ldots, 6$ with

$$A_\ell(\boldsymbol{\kappa}) = \mathcal{F} V_\ell(\boldsymbol{\rho}) = \frac{1}{2\pi} \int\!\!\int_{-\infty}^{\infty} V_\ell(\boldsymbol{\rho})\, \mathrm{e}^{-\mathrm{i}\boldsymbol{\kappa}\cdot\boldsymbol{\rho}}\, \mathrm{d}^2\rho\,. \tag{5.4}$$

- Next we conclude a propagation method $\boldsymbol{\mathcal{P}}$ on the basis of (5.3). To this end we consider the propagation problem of Eq. (5.2) for a single plane wave first.
- By that we benefit from the fact, that we know a plane wave as a 3D field alreday. A plane wave (member of the the subset with real valued $k_x$ and $k_y$ in which we are interested in) is given by $A_\ell\ \mathrm{e}^{\mathrm{i}\boldsymbol{\kappa}\cdot\boldsymbol{\rho}}\, \mathrm{e}^{\mathrm{i}\tilde{k}_z z}$.

- The plane wave field components at $z = 0$ are then given by

$$V_\ell(\boldsymbol{\rho}, 0) = A_\ell \;\, \mathrm{e}^{\mathrm{i}\boldsymbol{\kappa}\cdot\boldsymbol{\rho}}\, \mathrm{e}^{\mathrm{i}\tilde{k}_z \times 0} \tag{5.5}$$

  with the amplitudes $A_\ell$ of all component. The second exponential term is of course 1 in the plane with $z = 0$.

- In any plane $z > 0$ the plane wave has the form

$$V_\ell(\boldsymbol{\rho}, z) = A_\ell \;\, \mathrm{e}^{\mathrm{i}\boldsymbol{\kappa}\cdot\boldsymbol{\rho}}\, \mathrm{e}^{\mathrm{i}\tilde{k}_z z} \tag{5.6}$$

  with $\tilde{k}_z$ according to (here we even allow an imaginary refractive index part)

$$\tilde{k}_z = \sqrt{k_0^2(n + \mathrm{i}\beta)^2 - (k_x^2 + k_y^2)}\,. \tag{5.7}$$

- Obviously, the propagation effect for a plane wave is given by the multiplication with the phase factor $\mathrm{e}^{\mathrm{i}\tilde{k}_z z}$. That is valid for all six components.

- This result can be used in the SPW decomposition according to (5.3) of an arbitrary field and it follows directly

$$V_\ell(\boldsymbol{\rho}, z) = \frac{1}{2\pi} \int\!\!\int_{-\infty}^{\infty} A_\ell(\boldsymbol{\kappa})\, \mathrm{e}^{\mathrm{i}\boldsymbol{\kappa}\cdot\boldsymbol{\rho}}\, \mathrm{e}^{\mathrm{i}\tilde{k}_z z}\, \mathrm{d}^2\kappa \tag{5.8}$$

  to which we refer to as SPW propagation integral.

- For numerical reasons it is convenient to summarize the SPW propagation operator as follows using (5.4)

$$\begin{aligned} V_\ell(\boldsymbol{\rho}, z) &= \mathcal{P} V_\ell(\boldsymbol{\rho}, 0) \\ &= \mathcal{F}^{-1}\left\{ \left( \mathcal{F} V_\ell(\boldsymbol{\rho}, 0) \right) \mathrm{e}^{\mathrm{i}\tilde{k}_z z} \right\} . \end{aligned} \tag{5.9}$$

  using the definitions of the Fourier transformation and its inverse.

- On the basis of the Fast Fourier Transform (FFT) algorithm the SPW operator can be implemented by two FFT's.

- The operator can be applied componentwise for $\ell = 1, \ldots, 6$. However, in practice it is only done for $\ell = 1, 2$ and the other components are calculated on demand from the propagated two electric field components.

- The propagation operator for the $x$- and $y$-components are obviously identical and we have no crosstalk. Thus, the propagation matrix in homogeneous istropic media is of the diagonal type (see Eq. (3.4)).

- The SPW operator (5.9) solves the propagation in homogeneous media rigorously in an electromagnetic way. We can also say, that it delivers a solution of Maxwell's equations in 3D (positive half sphere) if the harmonic field is specified in a plane $\Upsilon$.

- In summary we can conclude, that an electromagnetic harmonic field in 3D can be constructed as follows:
  1. Choose arbitrary, square-integrable functions to define the $x$- and $y$-component of the electric field in the plane with $z = 0$.
  2. By applying Eq. (5.9) both components can be propagated into any plane with $z > 0$.
  3. All missing components can be calculated from the electric $x$- and $y$-components.
- Let us assume a globally polarized field, that means

$$V_\ell(\boldsymbol{\rho}, 0) = J_\ell \, U(\boldsymbol{\rho}, 0) \tag{5.10}$$

for $\ell = 1, 2$. Propagation of both components leads according to (5.9) to

$$V_\ell(\boldsymbol{\rho}, z) = J_\ell U(\boldsymbol{\rho}, z) = J_\ell \mathcal{F}^{-1}\left\{ \Big( \mathcal{F} U(\boldsymbol{\rho}, 0) \Big) \, \mathrm{e}^{\mathrm{i}\tilde{k}_z z} \right\} . \tag{5.11}$$

- Thus, the propagated field is still globally polarized, as it is typical for diagonal type matrix operators.

- It should be repeated and emphasized, that the characteristic of global polarization is only valid in the $xy$-projection plane of polarization observation. In the other planes we obtain local polarization.
- Next we discuss approximations of the SPW propagation operator.
- First of all that gives some more insight into propagation characteristics of harmonic fields.
- However, the approximations are also important from a numerical point of view. The SPW operator suffers from high numerical effort for propagating fields which are not very paraxial. For non-paraxial fields it is even often not practical to use SPW propagation at all.
- Explanation of high numerical effort for SPW operator for ~~l~~doing propagation distances and/or high divergent fields:
  - The field components to be propagated must be sampled. According to sampling theory the sampling period is reciprocally proportional to the bandwidth of the component.
  - The bandwidth is the extent of $\mathcal{F}V_\ell(\rho) = A_\ell(\kappa)$.

- According to Eq. (5.9) $A_\ell$ is multiplied with the phase factor $\mathrm{e}^{\mathrm{i}\tilde{k}_z z}$.
- Thus the extent of the resulting product is the same as the one of $A_\ell$. That means the bandwidth of the propagated field is the same one of the as the initial one.
- Fundamental conclusion: The sampling period is an invariant of free-space propagation!
- However, propagating fields become larger (at least after passing a focal point) and that means the required number of sampling points increases with propagation distance. That restricts the use of the SPW operator drastically in practice.

• VirtualLab$^{\mathrm{TM}}$ Illustration of SPW operator.

• Thus, there is a numerical demand for alternative operators, which may help to overcome the numerical problems with SPW propagation.

## 5.3 Fresnel propagation integral

- Mathematically the paraxial approximation is given by

$$\boldsymbol{\kappa}^2 = k_x^2 + k_y^2 << k_0^2 n^2 = k^2 \,. \tag{5.12}$$

- In this sense paraxial fields include only propagating plane waves with small spatial frequencies, which means nothing else than small angles.
- The paraxial approximation leads to an approximated expression of the $z$-component of the wave vector. Taylor expansion of

$$\tilde{k}_z(\boldsymbol{\kappa}) = \sqrt{k_0^2 n^2 - \boldsymbol{\kappa}^2} \,, \tag{5.13}$$

  for small $\boldsymbol{\kappa}^2$ up to the first order leads to

$$\tilde{k}_z(\boldsymbol{\kappa}) \approx k_0 n - \frac{\boldsymbol{\kappa}^2}{2k_0 n} \,, \tag{5.14}$$

  with the complex refractive index $n = n + \mathrm{i}\beta$ and $\boldsymbol{\kappa} = (k_x, k_y)$.
- The approximation replaces a spherical function $\tilde{k}_z(\boldsymbol{\kappa})$ by a parabolic one. This is illustrated in Fig. (8.6).

- Inserting this approximation into the SPW integral (5.8) leads to the integral

$$V_\ell(\boldsymbol{\rho}, z) = \frac{e^{ik_0nz}}{4\pi^2} \int\int_{-\infty}^{\infty} \left[ \int\int_{-\infty}^{\infty} V_\ell(\boldsymbol{\rho}') \, e^{-i\boldsymbol{\kappa}\cdot\boldsymbol{\rho}'} \, d^2\rho' \right] e^{i\boldsymbol{\kappa}\cdot\boldsymbol{\rho}} \, e^{-iz\frac{\boldsymbol{\kappa}^2}{2k_0n}} \, d^2\kappa \quad (5.15)$$

whereby

$$A_\ell(\boldsymbol{\kappa}) = \frac{1}{2\pi} \int\int_{-\infty}^{\infty} V_\ell(\boldsymbol{\rho}') \, e^{-i\boldsymbol{\kappa}\cdot\boldsymbol{\rho}'} \, d^2\rho' \quad (5.16)$$

was used.

- We rewrite the integral and obtain

$$V_\ell(\boldsymbol{\rho}, z) = \frac{e^{ik_0nz}}{4\pi^2} \int\int_{-\infty}^{\infty} V_\ell(\boldsymbol{\rho}') \left[ \int\int_{-\infty}^{\infty} e^{-iz\frac{\boldsymbol{\kappa}^2}{2k_0n}} \, e^{i\boldsymbol{\kappa}\cdot(\boldsymbol{\rho}-\boldsymbol{\rho}')} \, d^2\kappa \right] d^2\rho' \, . \quad (5.17)$$

- The inner integral can be understood as an inverse Fourier transformation of $e^{-iz\frac{\boldsymbol{\kappa}^2}{2k_0n}}$ with the conjugate variables $\boldsymbol{\kappa}$ and $(\boldsymbol{\rho} - \boldsymbol{\rho}')$.
- Fortunately this transformation can be performed analytically and one obtains

$$V(\boldsymbol{\rho}, z) = \frac{k_0n \, e^{ik_0nz}}{i2\pi z} \int\int_{-\infty}^{\infty} V(\boldsymbol{\rho}') \, e^{i\frac{k_0n}{2z}(\boldsymbol{\rho}-\boldsymbol{\rho}')^2} \, d^2\rho' \quad (5.18)$$

which we refer to as the Fresnel propagation integral in convolution form.

- By expanding the convolution term $\mathrm{e}^{\mathrm{i}\frac{k_0 n}{2z}(\boldsymbol{\rho}-\boldsymbol{\rho}')^2}$ we obtain

$$V_\ell(\boldsymbol{\rho}, z) = \alpha(\boldsymbol{\rho}, z)\,\frac{1}{2\pi}\int\!\!\int_{-\infty}^{\infty} V_\ell(\boldsymbol{\rho}')\ \mathrm{e}^{\mathrm{i}\frac{k_0 n}{2z}\boldsymbol{\rho}'^2}\ \mathrm{e}^{-\mathrm{i}\frac{k_0 n}{z}\boldsymbol{\rho}\cdot\boldsymbol{\rho}'}\ \mathrm{d}^2\rho' \tag{5.19}$$

with

$$\alpha(\boldsymbol{\rho}, z) = \frac{k_0 n}{\mathrm{i}z}\ \mathrm{e}^{\mathrm{i}k_0 n z}\ \mathrm{e}^{\mathrm{i}\frac{k_0 n}{2z}\boldsymbol{\rho}^2}\,. \tag{5.20}$$

- By the substitution $\boldsymbol{\beta} = \frac{k_0 n}{z}\boldsymbol{\rho}$ the second factor in (5.20) becomes $\mathrm{e}^{-\mathrm{i}\boldsymbol{\beta}\cdot\boldsymbol{\rho}'}$, which represents a Fourier transform kernel and it follows

$$V_\ell(\boldsymbol{\rho}, z) = \alpha(\boldsymbol{\rho}, z)\,\mathcal{F}_\beta\Big[V_\ell(\boldsymbol{\rho}')\ \mathrm{e}^{\mathrm{i}\frac{k_0 n}{2z}\boldsymbol{\rho}'^2}\Big]_{\boldsymbol{\beta}=\frac{k_0 n}{z}\boldsymbol{\rho}} \tag{5.21}$$

with the FT between $\rho'$ and $\beta$. By final substitution of $\boldsymbol{\beta} = \frac{k_0 n}{z}\boldsymbol{\rho}$ the desired propagated field component is obtained.

- The Fresnel integral (5.21) is of the factorized form

$$V_\ell(\boldsymbol{\rho}, z) \propto \mathrm{e}^{\mathrm{i}\frac{k}{2z}\boldsymbol{\rho}^2}\,V_\ell'(\boldsymbol{\rho}, z) \tag{5.22}$$

with

$$V'_\ell(\boldsymbol{\rho}, z) = \mathcal{F}_\beta^{\cancel{-1}} \left[ V_\ell(\boldsymbol{\rho}') \, \mathrm{e}^{\mathrm{i}\frac{k_0 n}{2z} \boldsymbol{\rho}'^2} \right]_{\boldsymbol{\beta} = \frac{k_0 n}{z} \boldsymbol{\rho}} . \tag{5.23}$$

- That allows the numerical calculation of $V'_\ell$ only and an analytical handling of the quadratic phase factor in (5.22). In comparison to $V_\ell$ the sampling of the function $V'_\ell$ is more relaxed for sufficiently large $z$. That is a big numerical advantage of the Fresnel integral in its form of eq. (5.21).
- The SPW operator is numerically efficient for small distances.
- The Fresnel operator is numerically efficient for larger distances.
- $\Longrightarrow$ For paraxial situations both operators together solve the propagation problem in practice.
- What is with the propagation of non-paraxial fields? See OMD I in summer.
- VirtualLab™ Illustration of SPW operator.

# Chapter 6

# Paraxial field tracing

## 6.1 Introduction

We distinguish between different versions of field tracing approaches, which all trace *electromagnetic fields* through optical systems:

- *General field tracing* utilizes the combination of any suitable propagation technique in different regions of the system. It takes maximum benefit from the capability for unified optical modeling by field tracing.
- *Paraxial field tracing* restricts to the application of the thin element approximation (TEA) to trace through components and Fresnel integral (or SPW) propagation through homogeneous media (free space regions). If the component effects are

restricted to parabolic phase effects, the complete system tracing can be described by the Collins integral. Paraxial field tracing constitutes a subset of general field tracing.

- *Gaussian beam tracing* provides analytical formulas for paraxial field tracing of Gaussian beams by the Collins integral. Because of that, it is extremely powerful to get fast results and analytical insight in tracing laser beams through lens system. However, it is restricted to paraxial modeling of lens systems.

- A paraxial field tracing analysis, maybe in combination with a ray tracing analysis, gives also in case of non-paraxial modeling situations often a helpful first insight into the optical function of a system.

- Paraxial modeling has the advantage of typically being numerically more efficient than non-paraxial approaches.

- For paraxial modeling tasks it is natural to use paraxial techniques.

- Paraxial concepts are often more intuitive for the blueprint of an optical system. See example of the thin lens in Sec. 4.2.2.

- In particular the design of light shaping systems, e.g. with diffractive optical elements, is typically based on paraxial modeling concepts.

- Finally, Gaussian beam tracing is very useful and popular to model and design paraxial lens systems for laser beams including resonator modeling.

## 6.2 Paraxial field tracing through lens systems

### 6.2.1 The Collins integral

- If we restrict to paraxial fields and parabolic phase effects on the fields by components, in fact that means lens systems, we can apply Collins integral for tracing fields through the system.

- The Collins integral follows from a combination of Fresnel's integral for free-space propagation and using TEA to model components. For spherical interfaces TEA results in a parabolic phase effect per interface according to Eq. (4.13).

- Obviously, the combination of TEA for components and physical optics for free space can be understood as a field tracing approach.

- In laser optics, Fourier optics, and various other fields of optics paraxial field tracing is a very popular and appropriate approach.

- Let us assume that the lens system is described by the matrix

$$\boldsymbol{\mathcal{M}}(\boldsymbol{\lambda}) = \begin{pmatrix} A(\lambda) & B(\lambda) \\ C(\lambda) & D(\lambda) \end{pmatrix} . \tag{6.1}$$

- It is emphasized, that in general the components are dependent on the wavelength of the field. In what follows this dependency is not explicitly shown.

- Next we assume the modeling through the lenses by TEA (see Sec. 4.2.2) and the free-space propagation between the lenses by the Fresnel intergal (see Eq. (5.21)).

- Obviously each modeling step introduces quadratic phase factors.

- By induction it can be proven that the resulting propagation integral of a paraxial field through the lens system is given by

$$V_\ell(\boldsymbol{\rho}, z) = \mathcal{P}_\mathrm{C} V_\ell(\boldsymbol{\rho}, 0) = \alpha(\boldsymbol{\rho}, z)\, \mathcal{F}_\beta \left[ V_\ell(\boldsymbol{\rho}', 0) \exp\left( \mathrm{i}\frac{k n_\mathrm{in} A}{2B} \boldsymbol{\rho}'^2 \right) \right]_{\boldsymbol{\beta} = \frac{k n_\mathrm{in}}{B} \boldsymbol{\rho}} \tag{6.2}$$

with

$$\alpha(\boldsymbol{\rho}, z) = \frac{k n_{\text{in}}}{\mathrm{i}B} \exp(\mathrm{i}kL) \exp\left(\mathrm{i}\frac{k n_{\text{out}} D}{2B}\boldsymbol{\rho}^2\right) . \tag{6.3}$$

where $L$ is the axial optical path length through the system.

- $n_{\text{in}}$ and $n_{\text{out}}$ represent the refractive indices in the input and output region of the system respectively. Often they are identical.

- Equation (6.2) uses the Fourier transformation

$$A_\ell(\boldsymbol{\kappa}) = \mathcal{F}V_\ell(\boldsymbol{\rho}) = \frac{1}{2\pi}\int\int_{-\infty}^{\infty} V_\ell(\boldsymbol{\rho})\,\mathrm{e}^{-\mathrm{i}\boldsymbol{\kappa}\cdot\boldsymbol{\rho}}\,\mathrm{d}^2\rho \tag{6.4}$$

but between $\rho'$ and $\beta$. By final substitution of $\boldsymbol{\beta} = \frac{k n_{\text{in}}}{B}\boldsymbol{\rho}$ the desired propagated field component is obtained.

- Next we turn to the inverse Collins integral, which transforms a propagated field back into the input plane.

- By resolving (6.2) for $V_\ell(\boldsymbol{\rho},0)$ we find the inverse Collins integral

$$V_\ell(\boldsymbol{\rho},0)=\mathcal{P}_{\mathrm{C}}^{-1}V_\ell(\boldsymbol{\rho},z)=\breve{\alpha}(\boldsymbol{\rho},z)\,\mathcal{F}_\beta^{-1}\left[V_\ell(\boldsymbol{\rho}',z)\,\exp\left(-\mathrm{i}\frac{kn_{\mathrm{out}}D}{2B}\boldsymbol{\rho}'^2\right)\right]_{\boldsymbol{\beta}=\frac{kn_{\mathrm{in}}}{B}\boldsymbol{\rho}} \tag{6.5}$$

with

$$\breve{\alpha}(\boldsymbol{\rho},z)=\frac{\mathrm{i}B}{kn_{\mathrm{in}}}\exp(-\mathrm{i}kL)\,\exp\left(-\mathrm{i}\frac{kn_{\mathrm{in}}A}{2B}\boldsymbol{\rho}^2\right). \tag{6.6}$$

### 6.2.2 Important ABCD matrices

- In what follows some matrices are given which are essential in paraxial field tracing as well as in Gaussian beam tracing.

- A free-space propagation ($n_{\mathrm{in}}=n_{\mathrm{out}}$) of distance $\pm a$ is given by the matrix

$$\boldsymbol{\mathcal{M}}_a=\begin{pmatrix}1 & \pm a\\ 0 & 1\end{pmatrix}. \tag{6.7}$$

- A spherical mirror with radius of curvature $R$ leads to the matrix

$$\boldsymbol{\mathcal{M}}_{\mathrm{SM}} = \begin{pmatrix} 1 & 0 \\ -\frac{2}{R} & 1 \end{pmatrix} . \tag{6.8}$$

- A spherical interface (radius of curvature $R$) between media of index $n_1$ and $n_2$ yields the matrix

$$\boldsymbol{\mathcal{M}}_{\mathrm{SI}} = \begin{pmatrix} 1 & 0 \\ \frac{n_1 - n_2}{n_2}\frac{1}{R} & \frac{n_1}{n_2} \end{pmatrix} \tag{6.9}$$

with the special case of a plane interface for $R = \infty$.

- A thin lens of focal length $f$ is represented by the matrix

$$\boldsymbol{\mathcal{M}}_{\mathrm{L}} = \begin{pmatrix} 1 & 0 \\ -\frac{1}{f} & 1 \end{pmatrix} . \tag{6.10}$$

- Next we turn to combined matrices. Of special importance is the combination of free space propagation steps $a$ and $b$ in front and behind a lens[1]. Combination of

[1]Here we assume $n = n_{\mathrm{in}} = n_{\mathrm{out}}$

(6.7) and (6.10) results in the matrix

$$\boldsymbol{\mathcal{M}}_{a\mathrm{L}b} = \boldsymbol{\mathcal{M}}_{\mathrm{b}}\boldsymbol{\mathcal{M}}_{\mathrm{L}}\boldsymbol{\mathcal{M}}_{\mathrm{a}} = \begin{pmatrix} 1-\frac{b}{f} & b+\frac{a}{f}(f-b) \\ -\frac{1}{f} & 1-\frac{a}{f} \end{pmatrix} . \tag{6.11}$$

- From that follows three important special cases:
  1. The $1f$-setup with $a = 0$ and $b = f$ yields
  $$\boldsymbol{\mathcal{M}}_{1f} = \begin{pmatrix} 0 & f \\ -\frac{1}{f} & 1 \end{pmatrix} . \tag{6.12}$$
  2. With $a = b = f$ we find the matrix for the $2f$-setup:
  $$\boldsymbol{\mathcal{M}}_{2f} = \begin{pmatrix} 0 & f \\ -\frac{1}{f} & 0 \end{pmatrix} . \tag{6.13}$$
  3. Finally the imaging equation $1/f = 1/a + 1/b$ results in the matrix
  $$\boldsymbol{\mathcal{M}}_{\mathrm{IMG}} = \begin{pmatrix} m & 0 \\ -\frac{1}{f} & 1/m \end{pmatrix} \tag{6.14}$$
  with the magnification $m = -b/a$.

### 6.2.3 Collins integral of special systems

- In what follows Eqs. (6.2) and (6.3) are considered for some special $ABCD$ matrices.

- Here we assume $z = 0$ indicates the input plane and $z$ the output plane. Moreover we assume $n = n_{\mathrm{in}} = n_{\mathrm{out}}$.

#### Free space propagation

- First we consider the simple propagation matrix (6.7) and obtain for $a = z$ the well-known Fresnel integral (compare with (5.21))

$$V_\ell(\boldsymbol{\rho}, z) = \alpha(\boldsymbol{\rho}, z)\, \mathcal{F}_\beta \left[ V_\ell(\boldsymbol{\rho}', 0)\, \exp\left( \mathrm{i}\frac{kn}{2z}\boldsymbol{\rho}'^2 \right) \right]_{\boldsymbol{\beta}=\frac{kn}{z}\boldsymbol{\rho}} \tag{6.15}$$

with

$$\alpha(\boldsymbol{\rho}, z) = \frac{kn}{\mathrm{i}z} \exp(\mathrm{i}knz)\, \exp\left( \mathrm{i}\frac{kn}{2z}\boldsymbol{\rho}^2 \right) \,. \tag{6.16}$$

**Fourier transforming systems**

- Next the $2f$-setup matrix (6.13) is used and we obtain

$$V_\ell(\boldsymbol{\rho}, z) = \alpha_{2f}\,\mathcal{F}_\beta\Big[V_\ell(\boldsymbol{\rho}', 0)\Big]_{\boldsymbol{\beta}=\frac{kn}{f}\,\boldsymbol{\rho}} \tag{6.17}$$

with

$$\alpha_{2f} = \frac{kn}{\mathrm{i}f}\exp(\mathrm{i}2knf)\,. \tag{6.18}$$

Obviously besides a constant factor $\alpha$ the $2f$-setup performs a Fourier transform.

- The $1f$-setup leads to a slightly different result, that is

$$V_\ell(\boldsymbol{\rho}, z) = \alpha(\boldsymbol{\rho}, f)\,\mathcal{F}_\beta\Big[V_\ell(\boldsymbol{\rho}', 0)\Big]_{\boldsymbol{\beta}=\frac{kn}{f}\,\boldsymbol{\rho}} \tag{6.19}$$

and

$$\alpha(\boldsymbol{\rho}, f) = \frac{kn}{\mathrm{i}f}\exp(\mathrm{i}knf)\,\exp\left(\mathrm{i}\frac{kn}{2f}\boldsymbol{\rho}^2\right)\,. \tag{6.20}$$

- That means, in a $1f$-setup a quadratic phase remains on the field in the output plane.

- With (6.11) and $a \neq f$ and $b = f$ we have a more general result, which contains the $1f$- and $2f$-setup as special cases. We find the propagation operator

$$V_\ell(\boldsymbol{\rho}, z) = \alpha(\boldsymbol{\rho}, z)\, \mathcal{F}_\beta \Big[ V_\ell(\boldsymbol{\rho}', 0) \Big]_{\boldsymbol{\beta} = \frac{kn}{f} \boldsymbol{\rho}} \tag{6.21}$$

with

$$\alpha(\boldsymbol{\rho}, z) = \frac{kn}{\mathrm{i}f} \exp(\mathrm{i}kn\,(a+f))\, \exp\left( \mathrm{i}\frac{kn(1-a/f)}{2f} \boldsymbol{\rho}^2 \right) . \tag{6.22}$$

- Thus, independent of the distance of the input plane from the lens a Fourier transformation is performed by the lens multiplied with a quadratic phase factor. For $a = f$ this factor disappears. We conclude, that any system with the matrix

$$\boldsymbol{\mathcal{M}}_{aff} = \begin{pmatrix} 0 & f \\ -\frac{1}{f} & 1 - a/f \end{pmatrix} \tag{6.23}$$

represents a Fourier transforming system with the special cases for $a = 0$ and $a = f$.

**Imaging**

- Finally the imaging matrix (6.14) is discussed.

- Because of $B = 0$ the Collins integral must be discussed for the limit $1/B \to \infty$ which results for $n = 1$ in

$$V_\ell(\boldsymbol{\rho}, z) = \frac{\operatorname{sign}(m)}{m} \exp[\mathrm{i}k(a+b)] \exp\left(-\mathrm{i}\frac{k}{2mf}\boldsymbol{\rho}^2\right) V_\ell(\boldsymbol{\rho}/m, 0)\,. \tag{6.24}$$

- The quadratic phase term vanishes for large $f$.
- It should be noted, that (6.24) also gives the result for the special case of a single lens and $a = b = 0$ and $m = 1$. Then the field multiplied with the parabolic phase factor remains, which is the expected result when TEA is applied for the lens.

## 6.3 Gaussian beam tracing

Here we continue in Optical Modeling and Design I.

Besides OMD I the lecture “Physical optics simulations with VirtualLab” will be given, both in P1100 of Multimedia Center. I’ll send to you more information before April.

# Chapter 7

# VirtualLab$^{\mathrm{TM}}$ simulations

## 7.1 Electric field illustration

*B.00_Field.Components.lpd*:

1. Short introduction to VirtualLab$^{\mathrm{TM}}$ sources at example Gaussian.
2. Linear polarization 1 degree divergence: $x, y, z$-components.
3. Linear polarization 25 degrees divergence: $x, y, z$-components.
4. Change to circular polarization: $x, y, z$-components.
5. Donut mode: $x, y, z$-components.

## 7.2 Magnetic field illustration

*B.00_Field.Components.lpd*:

1. Linear polarization 25 degrees divergence: $x, y, z$-components.
2. Change to circular polarization: $x, y, z$-components.
3. Donut mode: $x, y, z$-components.

## 7.3 Polarizaion illustration

*B.00_Field.Components.lpd*:

1. Linear polarization 1 degree divergence: polarization in all projection planes.
2. Change to circular polarization: polarization in all projection planes.
3. Increase divergence to 30 degrees: polarization in all projection planes.
4. Donut mode: polarization in $xy$-plane.

## 7.4 Polarization effects by free-space propagation

*B.00_Field.Components.lpd*:

1. Circular polarization 1 degree divergence: polarization in all projection planes.
2. Circular polarization 1 degree divergence; 10 mm propagation: polarization in all projection planes.
3. Increase divergence to 20 degrees: polarization in all projection planes; keep result.
4. Propagation 10 $\mu$m: polarization in all projection planes; compare with $z = 0$.
5. *B.01_Scattering_rough_surface.lpd*: Without discussion of TEA show field behind scatterer and then free space propagation effect for donut mode source.

## 7.5 Polarization effects by generalized Jones matrices

*VLD_General.Jones.Matrix_Illustration.1.lpd* and *VLD_General.Jones.Matrix_Illustration.2.lpd*:

1. General Jones matrix 1 rotates local polarization
2. Discuss effects for different inputs: linear $x$-polarization, 45 degrees, circular polarization
3. Show also electric field components.
4. Same for matrix 2.
5. Here also amplitude effects.

## 7.6 Polarization effects by Jones matrices

*VLD_Jones.Matrix_Illustration.lpd*:

1. Discuss system. No effect for linear $x$-polarization.
2. Rotate polarizer by position tab rotation around $z$-axis: reduced amplitude follows.
3. 45 degrees polarization in input.
4. Change to retarder.
5. Donut mode

## 7.7 Illustration of SPW operator

1. Major window: default plane wave; 100 mm; effort check
2. Major window: default Gaussian; 100 mm; effort check
3. Major window: Gaussian 5 degrees; 100 mm; effort check

## 7.8 Illustration of Fresnel operator

*F.01a_Automatic.Selection_Diffraction.lpd*

- Gaussian 1 degree; 100 mm, 1 $\mu$m; check SPW + Fresnel
- Super Gaussian 100 $\mu$m; 100 mm; check SPW + Fresnel
- LPD diffraction experiment: 2D 0-100 mm, 20 steps, parameter run
- LPD diffraction experiment: 1D 0-70 mm, 50 steps, parameter run

# Chapter 8

# Figures


Figure 8.1: Example of optical system.

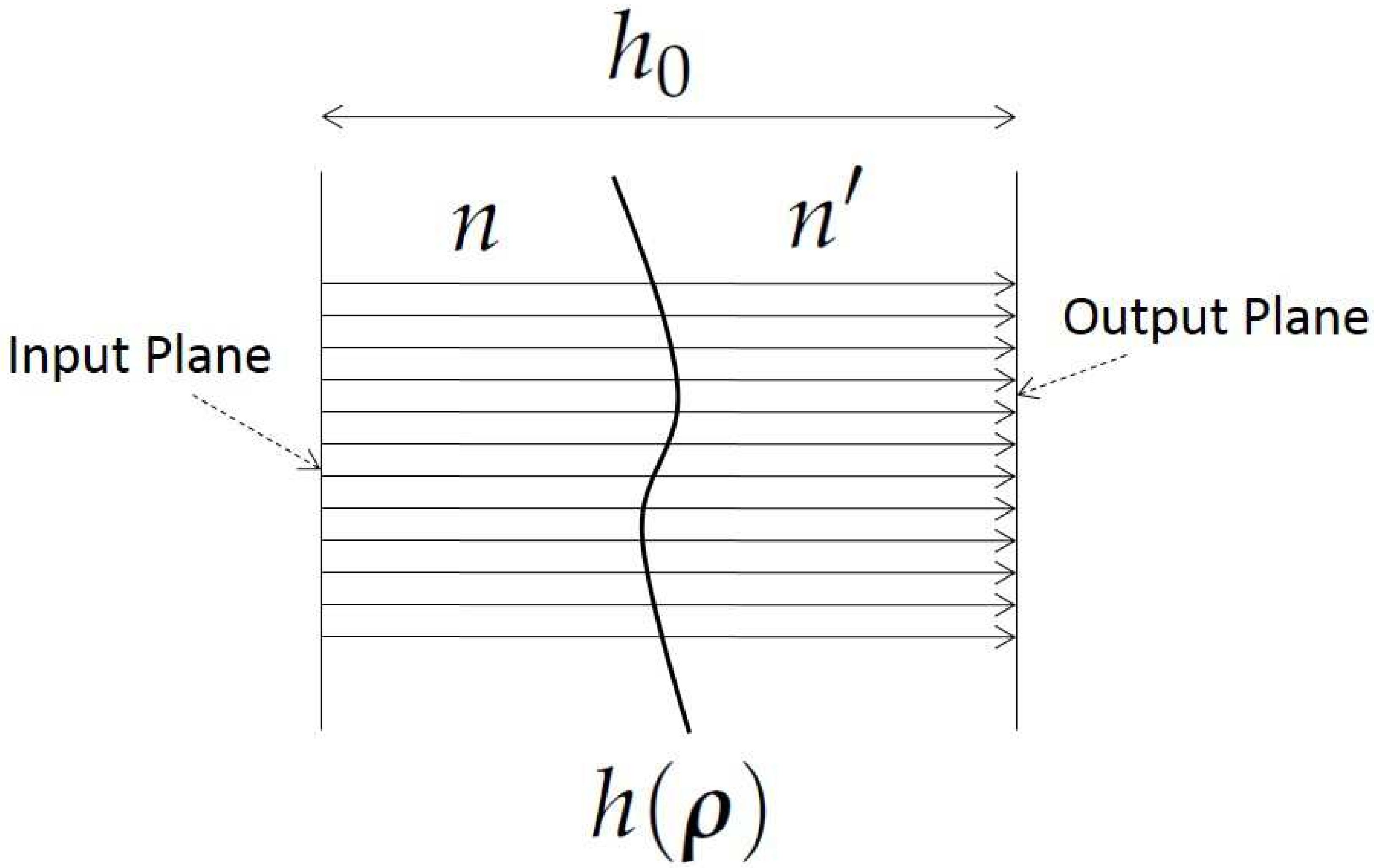


Figure 8.2: Illustration of the propagation through a single interface with the height profile $h(\boldsymbol{\rho})$ by the thin element approximation.

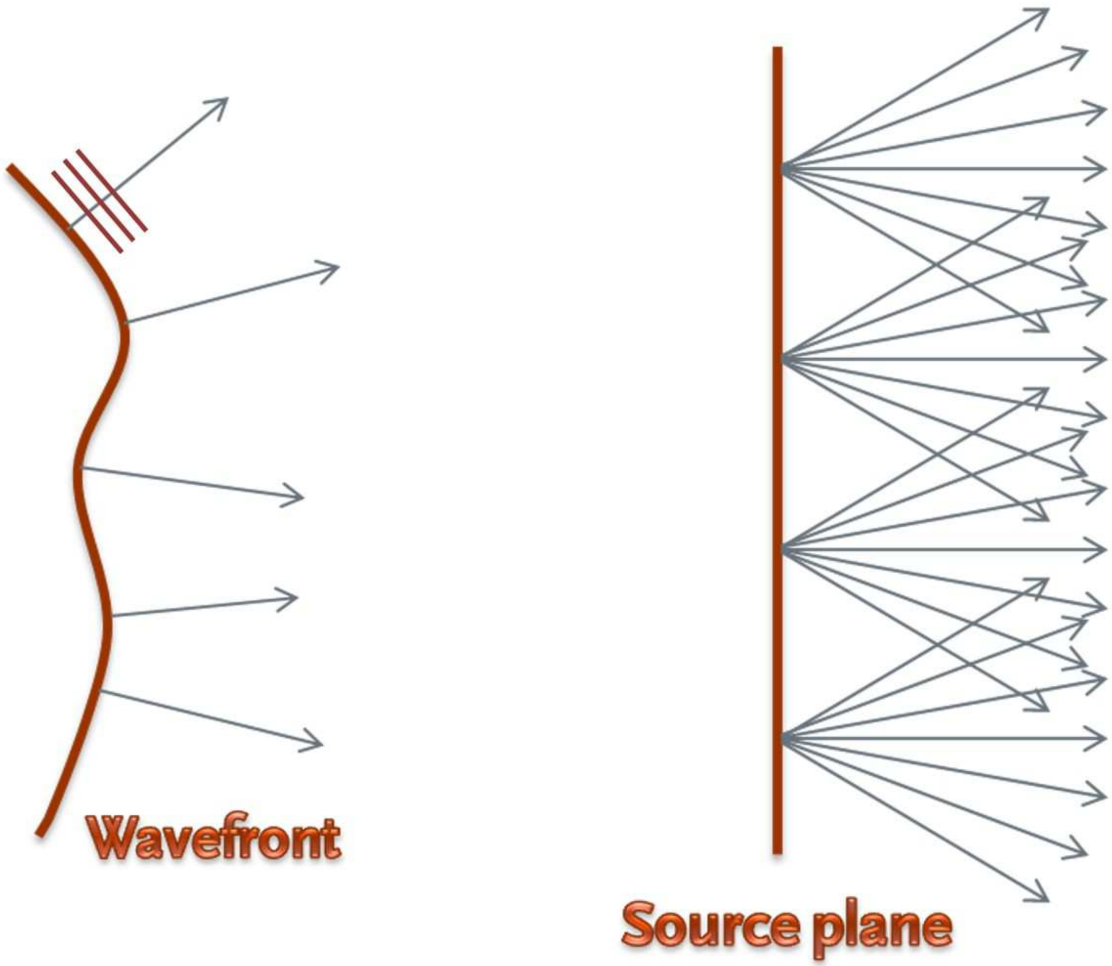


Figure 8.3: Illustration of LPWA.

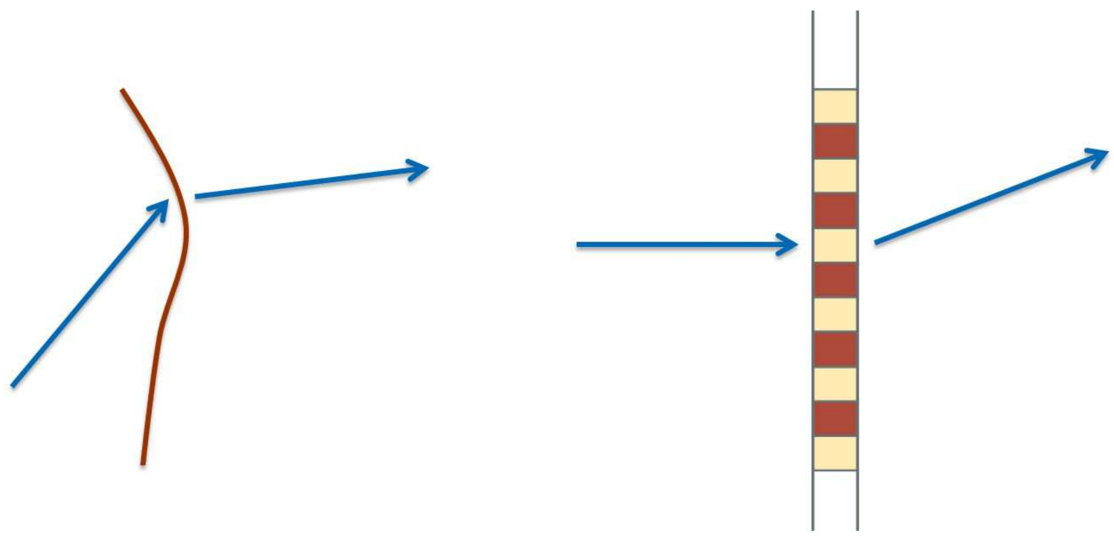

Figure 8.4: Illustration of LPIA and LLGA.

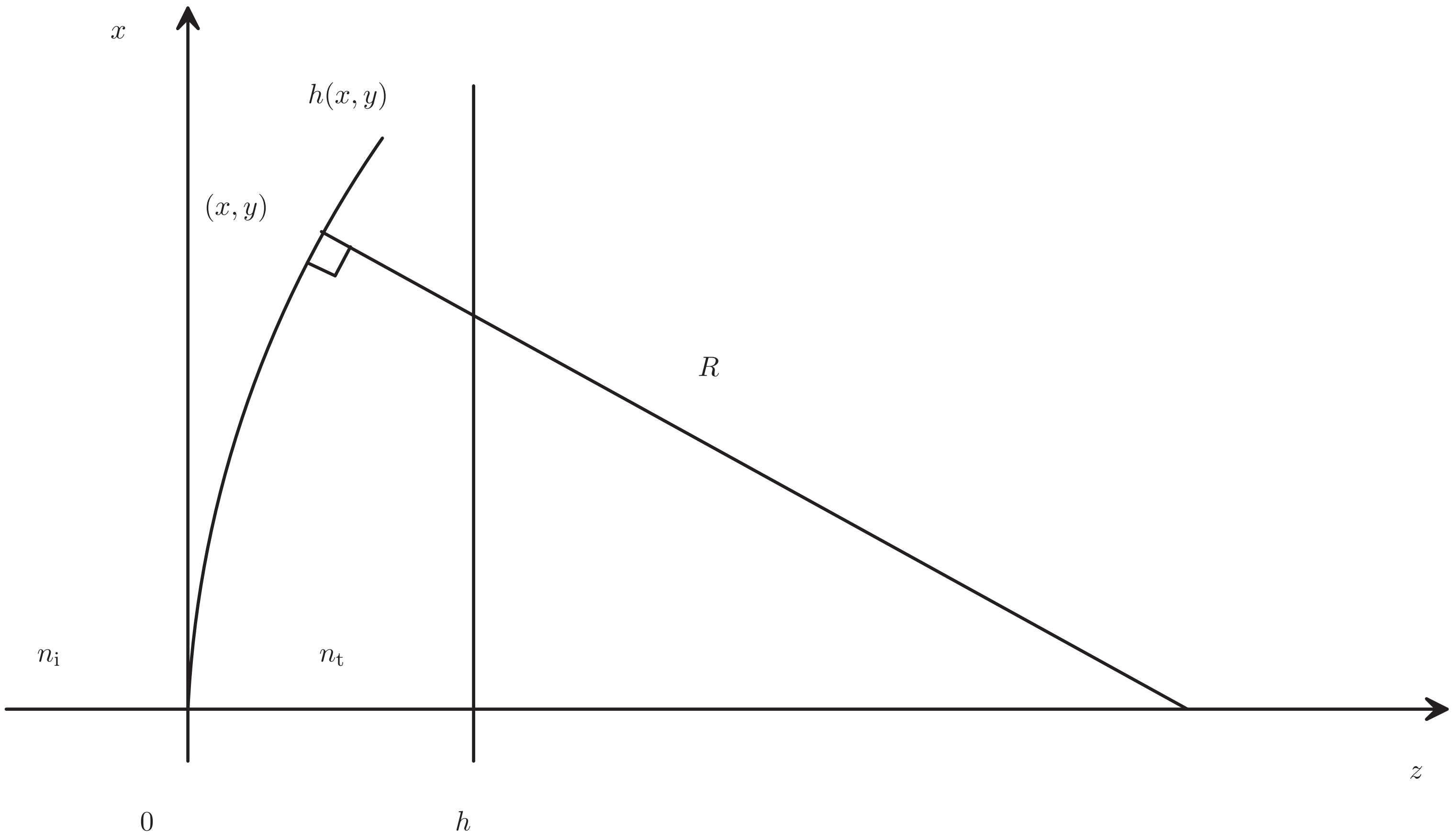


Figure 8.5: Illustration of a spherical interface with a positive radius of curvature $R$ between two homogeneous media. Here we use the indices i and t for the input and output fields.

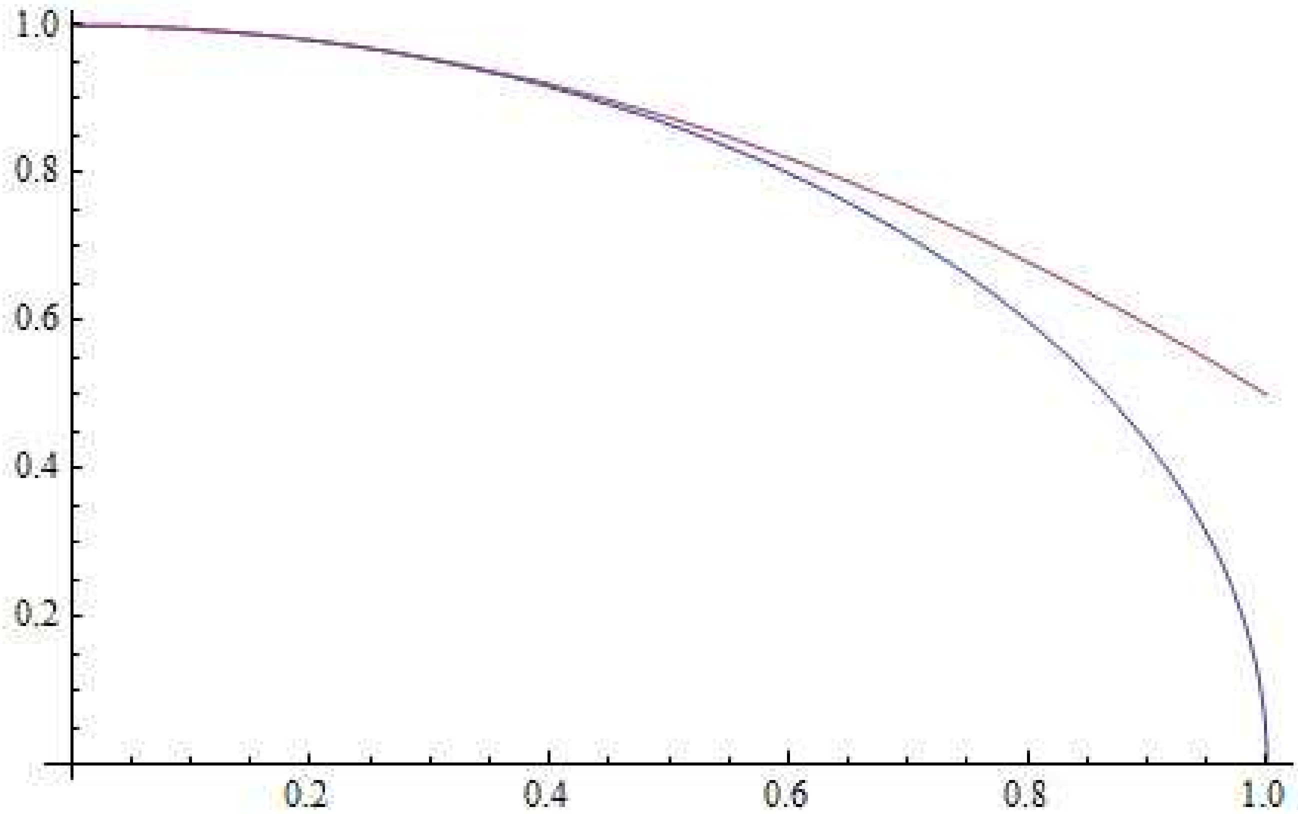


Figure 8.6: Illustration of paraxial approximation: The blue line illustrates the correct spherical phase of the SPW propagation kernel. The red line shows this phase in its paraxial approximation. Both curves are close together up to $k_x \approx .5$.